ISBN: 978-3-95450-241-7 ISSN: 2673-5350 doi:10.18429/JACoW-IBIC2022-WEP28

STUDIES ON RADIALLY COUPLED FAST FARADAY CUPS TO MINIMIZE FIELD DILUTION AND SECONDARY ELECTRON EMISSION AT LOW INTENSITIES OF HEAVY IONS*

G. Rodrigues[1,†], K. Mal[1]. S. Kumar[1], R. Singh[2], C.P. Safvan[1], R. Mehta[1]
[1]Inter University Accelerator Centre, Aruna Asaf Ali Marg, New Delhi, India
[2]GSI Helmholtzzentrum fur Schwerionenforschung GmbH, Darmstadt, Germany

Abstract

Fast Faraday Cups (FFCs) are interceptive beam diagnostic devices used to measure fast signals from sub-nanosecond bunched beams and the operation of these devices is a well-established technique. However, for short bunch length measurements in non-relativistic regimes with ion beams, the measured profile is diluted due to field elongation and distortion by the emission of secondary electrons. Additionally, for short bunches with a low "signal to noise ratio" envisaged in the High Current Injector at the Inter University Accelerator Centre, the impedance matching of the EM structure puts severe design constraints. This work presents a detailed study on the modification of a radially-coupled coaxial FFC. The field dilution and secondary electron emission aspects are modelled through EM simulations and techniques to minimise these effects are explored.

INTRODUCTION

In the upcoming High Current Injector (HCI) Programme [1, 2] at New Delhi, India, there is an urgent need for developing diagnostics for longitudinal measurements which are critical for the successful operation of the High Current Injector. The operation of Faraday cups for intensity measurements is well established where the suppression of the emitted secondary electrons is carried out using a superimposed electric field, such that the emitted secondary electrons are retarded and recaptured [3]. For longitudinal charge profile measurements of short bunches (≤ 5 ns), it is critical to avoid impedance discontinuities in the Faraday cup structure until frequencies up to few GHz. Modified Faraday cup designs tailored to measure longitudinal charge distributions [3, 4] are called Fast Faraday Cups (FFC) [5]. Early FFC designs were tapered extension of coaxial cables allowing for full beam deposition on the central conductor while maintaining 50 Ω characteristic impedance [3, 6]. Following that, alternative FFC designs based on radial coupling in the central conductor [5] of a co-axial cable and microstrip based designs [4, 7] have been used in various accelerator laboratories. Recently [8], two FFC designs, one using a Radially-Coupled Coaxial Fast Faraday Cup (RCFFC) and a conventionally axially coupled FFC (ACFFC) were simulated with ion beams and compared with the measurements under similar beam conditions. A strong distortion in the longitudinal charge profile measurement due to secondary electrons is observed. External DC biasing of the central conductors minimises the distortion to a large extent. Most studies available in the literature are focused mainly on electromagnetic characteristics, i.e. targeting impedance mismatch aspects. However, there are additional challenges for short bunched beam measurements in non-relativistic regimes; a) the field elongation and b) distortion by the emission of secondary electrons. In this study, we will present a design modification of a Radially-Coupled Coaxial Fast Faraday Cup (RCFFC) considering the existing beam conditions at the High Current Injector Programme, which is presently under commissioning stages at the Inter-University Accelerator Center (IUAC), New Delhi. The primary drawback of the original design is the low "signal-to-noise" ratio due to the narrow beam limiting aperture of 0.8 mm along with the need for precise beam alignment with long averaging times for the measurement. The second challenge is the delayed signal induction due to emission of secondary electrons. The major modifications in our adapted design is to counter these challenges and are discussed in this contribution.

EM SIMULATIONS OF A MODIFIED RCFFC

The characteristic impedance (Z_{coax}) of a coaxial transmission line is defined with the following parameters [9], ε and μ as the permittivity and permeability of the material respectively, with r_1 and r_2 being the radii of the inner and outer conductor, respectively. The non-TEM mode with the lowest cut-off frequency (f_c) is TE_{11} and the cut-off frequency given by the standard known relation. Since the width of the co-axial line cannot be arbitrarily increased, a conical taper between a thin and a thick co-axial line was chosen. In order to minimise the reflection at the transition of coaxial and conical lines, it is necessary to design in such a way that the characteristic impedances of both the lines have the same impedance of 50 Ω. CST Microwave Studio [10] was used to design the RCFFC assembly with the interfacing option to the transmission line at the desired characteristic impedance of 50 Ω. Figure 1 shows the cross-sectional view of the model of the RCFFC, which consists of a metallic cube with two N-type connectors positioned concentrically. The collimating aperture of diameter 2 mm is chosen based on the relatively lower beam intensities of heavy ions available at the upcoming, High Current Injector Programme. A rod of diameter 6 mm was inserted between the central electrodes of the connectors and tapered down to 3 mm, being the diameter of the standard N-type connector pin.

* Work supported by VAJRA
† gerosro@gmail.com

ISBN: 978-3-95450-241-7 ISSN: 2673-5350 doi:10.18429/JACoW-IBIC2022-WEP28

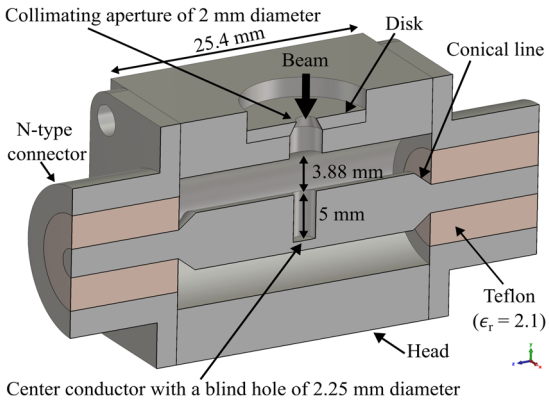

Figure 1: Model (cross-sectional view) of the RCFFC with the geometrical parameters

The rod acts as a collector as well as the transmission line's inner electrode. The diameter of the collector hole was chosen to be 2.25 mm to avoid hitting the beam directly. With these chosen dimensions, the first-order estimate of the RCFFC geometry parameters has been calculated using the analytical formula. For the chosen dimensions and the medium properties, the cut-off frequencies of the N-type connector and RCFFC head are 10.10 GHz and 9.64 GHz, respectively. In order to obtain the return loss (S_{11}) and insertion loss (S_{21}), a two-port analysis [11] was carried out by assigning two waveguide ports at the left and right N-type connectors; a Time Domain Reflection (TDR) [12] analysis was also performed to compute the distributed characteristic impedances along the coaxial and conical lines of the RCFFC.

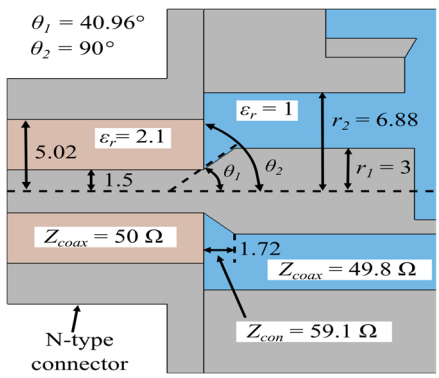

Figure 2: RCFFC geometry and its design parameters (unit: mm) for characteristic impedance of 50 Ω, with optimized design using CST-Microwave Studio.

The EM wave simulation was performed by considering only TEM mode at the waveguide ports with a frequency range up to 9 GHz to evaluate the performance. It was observed that the return loss of the RCFFC depicts two resonance peaks below the cut-off frequency (10.10 GHz) which are due to impedance mismatch at the conical lines and the center of the RCFFC, although, the insertion loss is not so large. Similarly, the characteristic impedance of the RCFFC is almost equal to theoretical impedance (50 Ω) but it also shows two capacitive peaks at the conical line and one inductive peak at the center of the RCFFC. The difference between the theoretical and simulated impedance at the conical line could possibly be due to the short length of the conical line. The inductive peak at the center of the RCFFC is due to the holes in the collector electrode and in the head of the RCFFC. To achieve uniform impedance and minimize the reflections at the junction between the conical and coaxial lines, the length of the conical line and inner radius of the outer conductor (r_2) were optimized. The optimized geometry parameters are shown in Fig. 2 where the length of the conical line is 1.72 mm and thus, the angle (θ_1) of the inner conductor of the conical line turns out to be 40.96°. The optimized inner radius (r_2) of the outer conductor is 6.88 mm to suppress the inductive peak at the center of the RCFFC. The theoretical characteristic impedance of the conical line and head of the RCFFC are 59.1 Ω and 49.8 Ω, respectively. The simulated return loss, insertion loss and characteristic impedance of the optimized geometry are shown in Fig. 3. and the return loss has been reduced from −30 dB to −55 dB. The insertion loss for the optimized geometry is also reduced. The impedance difference between the conical and coaxial lines was also significantly reduced and is almost equal to 50 Ω (see Fig. 3(b)). We can see that the insertion loss of the optimized RCFFC geometry attains a value of −0.005 dB at frequency 9 GHz. Using the well know relation between the bandwidth and the signal rise time, the rise time of the RCFFC geometry can be improved to a value better than 39 ps.

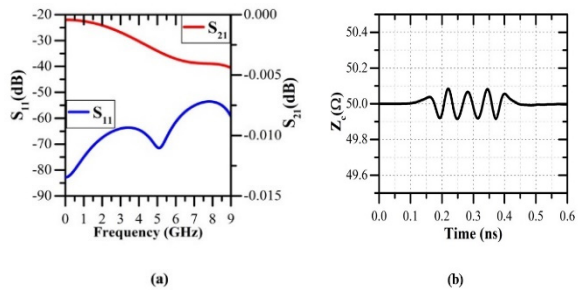

Figure 3: Simulated results of the optimized geometry, depicting (a) return loss at the input port, and insertion loss between two ports, (b) characteristic impedance (Z_c).

ROBUSTNESS OF THE DESIGN PARAMETERS

The effect of the manufacturing tolerances of the various parameters on the characteristic impedance of the RCFFC is further investigated. The diameter of the collector electrode ($d = 2r_1$), inner diameter of the outer conductor ($D = 2r_2$) and the transition length (L_{cone}) of coaxial to conical were increased by 0.1 mm individually about their optimized values (see Fig. 2). Figures 4(a) and 4(b) show the simulated reflection coefficient and the characteristic impedance of the RCFFC, respectively, when the diameter of the collector electrode (d), inner diameter of the outer conductor (D), and the transition length (L_{cone}) of the coaxial to conical line were increased by 0.1 mm.

For the sake of comparison, the reflection coefficient and the characteristic impedance for the optimal parameter values are also shown Fig. 4. It can be seen that a small change of 0.1 mm in the dimensions of the RCFFC causes significant changes in the reflection coefficient and characteristic

ISBN: 978-3-95450-241-7 ISSN: 2673-5350 doi:10.18429/JACoW-IBIC2022-WEP28

impedance, especially for the collector electrode. Therefore, these tolerances must be carefully considered during fabrication of the collector electrode.

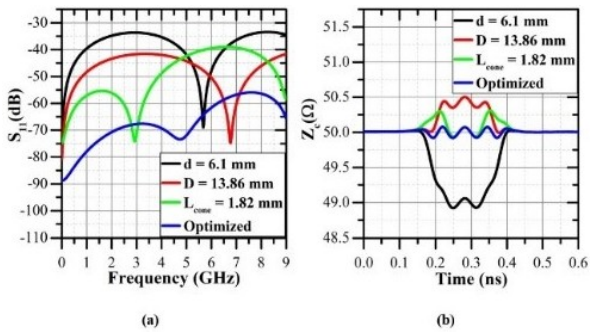

Figure 4: Simulated results showing the effect of individual tolerance on (a) Reflection coefficient and (b) Characteristic impedance of the RCFFC, when parameters are increased by 0.1 mm about their optimal values (d = 6 mm, D = 13.77 mm, and L_{cone} = 1.72 mm).

For the sake of comparison, the reflection coefficient and the characteristic impedance for the optimal parameter values are also shown Fig. 4. It can be seen that a small change of 0.1 mm in the dimensions of the RCFFC causes significant changes in the reflection coefficient and characteristic impedance, especially for the collector electrode. Therefore, these tolerances must be carefully considered during fabrication of the collector electrode.

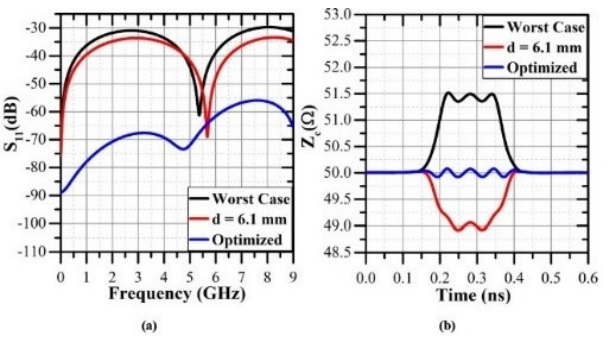

Figure 5: Simulated results showing the effect of tolerance on (a) Reflection coefficient and (b) Characteristic impedance of the RCFFC, for the worst case, for the case when d = 6.1 mm, and for the optimized parameters (d = 6 mm, D = 13.77 mm, and L_{cone} = 1.72 mm).

Let us consider the worst case, when all the dimensions of the RCFFC are off by 0.1 mm from their optimized values (d = 5.9 mm, D = 13.8 mm, and L_{cone} = 1.82 mm). Figure 5 shows the simulated reflection coefficient and characteristic impedance for the worst case, when the diameter of the collector electrode is only changed by 0.1 mm and for remaining optimal parameter values. From Fig. 5(a), a small change in the reflection coefficient is observed for the worst case compared to the case when the diameter of the collector electrode was changed by 0.1 mm alone. This further shows that how tight manufacturing tolerance is required for the collector electrode. Therefore, a margin of ± 0.1 mm is left to account for the manufacturing tolerances in order to obtain the reflection coefficient equal to −30 dB.

EMISSION OF SECONDARY ELECTRONS

Besides characteristic impedance, other properties need to be considered in design of the FFC for measuring bunch widths very accurately. In order to suppress all the SEs, electrostatic suppression is normally used in many conventional FCs [13–15] and FFCs [5, 16]. In our design, the electrostatic suppressor cannot be implemented in front of the collector electrode due to space constraints, therefore the blind hole structure in the collector itself , was modified. In order to minimise the losses of the SEs, their production mechanism, energy and angular distribution as well as the total yield (as a function of ion energy) are required. The energy distribution of the secondary electrons has a peak at few eV with a full width at half maximum (FWHM) of the same order of magnitude, thus about 80-95% of the ejected electrons are below 50 eV [17]. In order to stop the projectile ions of total energy 1.8 MeV/A, the thickness of the beam stopper should be much larger than the range of the projectiles. Copper material was chosen for the collector of the RCFFC because of its good electrical property and its excellent thermal conductivity. The range of ^{14}N ions of energy 25.2 MeV in copper has been calculated to be 8.2 µm using SRIM code [18] and similarly the range of ^{238}U of energy 428.4 MeV was found to be 12.7 µm. Thus, choosing a thickness of 1 mm is sufficient to stop all ions having energy of 1.8 MeV/A.

BUNCH LENGTH SIMULATIONS

The PIC solver of CST Microwave Studio calculates the EM fields and particle motion at discrete time samples. A Gaussian shaped longitudinal charge distribution with a beam bunch charge of 1 fC was used as the excitation source. signals at the N-type connectors, a short bunch length of σ = 13.5 ps with tails cut at 4σ and approximates 108 ps full width (8σ) was chosen to demonstrate the transient FFC signal induction process. For such a bunch travelling with velocity corresponding to β = 0.06, the full width of the bunch is approximately 2 mm which is less than the blind hole depth of (5 mm) in the collector electrode. The head of the RCFFC was maintained at ground potential and the inner conductor which acts as collector was at the floating potential. The beamlet formed by the aperture of diameter 2 mm in the collimation disk travels through a gap of length L = 3.88 mm between the grounded body and the collector electrode, and is absorbed within a blind hole situated inside the collector electrode. Figure 6(a) demonstrates the propagation of a Gaussian pulse, while Figs. 6(b) and 6(c) show respectively the induced surface current density and the induced voltage signal on one of the N-type connector. The time (x-axis) in Fig. 6(c) is translated by 94 ps to account for the wave traversal from center of the FFC to one of the N-type connectors. As it can be seen, the voltage signal starts to induce once the bunch starts to enter the gap and rises as the bunch approaches the

ISBN: 978-3-95450-241-7 ISSN: 2673-5350 doi:10.18429/JACoW-IBIC2022-WEP28

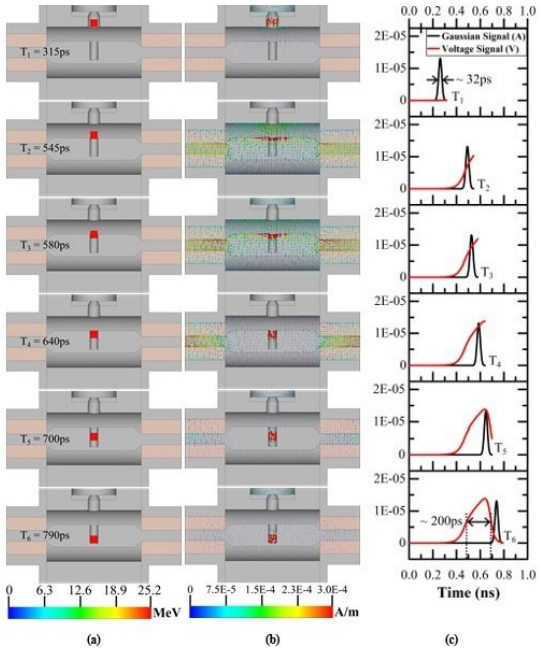

Figure 6: Simulation of a Gaussian pulse having bunch length $\sigma = 13.5$ ps with $\beta = 0.06$ through the RCFFC showing (a) Propagation of a Gaussian bunch; (b) induced surface current density; and (c) induced voltage signal on one of the N-type connectors and a Gaussian pulse.

collector electrode. The induced signal attains the highest value (at time $T_2 = 545$ ps), when the bunch is about to enter in the blind hole of the collector electrode. At this point ($T_2 = 545$ ps), the maximum density of the opposite charges (electrons) induces on the collector electrode (see Fig. 6(b) and the same density of the electrons travels with the bunch when bunch starts to enter into the blind hole. As a result, the signal starts to reduce and reaches zero at time $T_5 = 700$ ps (see Fig. 6(c) before absorbing the bunch into the collector electrode where negative charges are neutralised with the positive charges of the bunch. Also, from Fig. 6(b), after time $T_4 = 640$ ps, there is no flow of current from centre of the FFC to the N-types connectors except the earlier induced current. That means the induced signal should be reduced to zero once the bunch completely entered into the hole, while it had reduced to zero at time $T_5 = 700$ ps and the full width at half maximum (FWHM = $2.3548\,\sigma$) of the induced signal is approximately 200 ps. The modelling shows that the bunch length of the induced signal will be $\sigma_c = 85$ ps which is larger than the bunch length of the input beam ($\sigma_b = 13.5$ ps).

CONCLUSION

The radially coupled coaxial FFC (RCFFC) design for high intensity proton beams is modified for low intensity ion beams. The central conductor and the hole for the beamlet entry were widened while maintaining the characteristic impedance of the full structure close to 50 Ω. A transition method without curved structures was adopted for the transition from the N-type connector to the cup region to achieve uniform impedance and low reflection. Adaptations in the shape of the blind hole surface in the central conductor was made to reduce the number of secondary electrons exiting the blind hole. Signal induction procedure and its dependence on the FFC design parameters, like entry hole size and gap length was discussed in detail. The effect of secondary electron emission on the induced signal is studied and potential remedy is proposed.

ACKNOWLEDGEMENT

R. Singh and G. Rodrigues would like to acknowledge the help and support received from the Department of Science and Technology (DST) related to the VAJRA project (VJR/2018/000115).

REFERENCES

[1] A. Roy, "Accelerator development at the Nuclear Science Centre", *Current Science*, vol. 76, pp. 149–153, 1999. http://www.jstor.org/stable/24101229

[2] D. Kanjilal *et al.*, "High Current Injector at Nuclear Science Centre", in: *Proc. APAC'04*, Gyeongju, Korea, Mar. 2004, paper MOP10008, pp. 73-75. https://jacow.org/a04/papers/mop10008.pdf

[3] P. Strehl, *Beam Instrumentation and Diagnostics*, Springer Verlag, Berlin Heidelberg, 2006.

[4] W. R. Rawnsley *et al.*, "Bunch shape measurements using fast Faraday cups and an oscilloscope operated by LabVIEW over Ethernet", *AIP Conf. Proc.*, vol. 546, p. 547, 2000. doi:10.1063/1.1342629

[5] J.-P. Carniero *et al.*, "Longitudinal beam dynamics studies at the PIP-II injector test facility", *Int. J. Mod. Phys. A.*, vol. 34, no. 36, 2019. doi:10.1142/S0217751X19420132

[6] H. Chuaqui *et al.*, "Simple Faraday cup with subnanosecond response", *Rev. Sci. Instrum.* vol. 60, p. 141, 1989. doi:10.1063/1.1140572

[7] M. Bellato *et al.*, "Design and tests for the fast Faraday cup of the ALPI post-accelerator", *Nucl. Instrum. Methods Phys. Res., Sect. A,* vol. 382, p. 118, 1996. doi:10.1016/S0168-9002(96)00508-6

[8] R. Singh *et al.*, "Simulation and Measurements of the Fast Faraday Cups at GSI UNILAC", in Proc. IBIC'22, Krakow, Poland, 2022.

[9] D M. Pozar, *Microwave engineering*, 2nd Edition, 1998 John-Wiley & Sons.

[10] www.3ds.com/cst-studio-suite/

[11] S. Y. Liao, *Microwave Devices and Circuits*, Prentice Hall, New Jersey, USA, 1985.

[12] https://space.mit.edu/RDIO/CST_online/mergedProjects/3D

[13] J.D. Thomas *et al.*, "Performance enhancement study of an electrostatic Faraday cup detector", *Nucl. Instrum. Meth. Phys. Res., Sect. A,* vol. 536, pp. 11–23, 2005. doi:10.1016/J.NIMA.2004.07.211

[14] E. Ebrahimibasabi and S.Feghhi, "Design and construction of a secondary electron suppressed Faraday Cup for measurement of beam current in an electrostatics proton accelerator", *Int. J. Mass Spectrom.* vol. 386, pp. 1–5, 2015. doi:10.1016/j.ijms.2015.05.006

[15] Cantero *et al.*, "Design of a compact Faraday cup for low energy, low intensity ion beams", *Nucl. Instrum. Methods Phys. Res., Sect. A,* vol. 807, pp. 86–93. doi:10.1016/J.NIMA.2015.09.096

ISBN: 978-3-95450-241-7 ISSN: 2673-5350 doi:10.18429/JACoW-IBIC2022-WEP28

[16] J. V. Mathew and A. Bajaj, "An improved strip-line fast Faraday cup for beam bunch measurements", *Rev. Sci. Instrum*., vol. 91, p. 113305, 2020. doi:10.1063/5.0025457

[17] D. Hasselkamp, S. Hippler, and A. Scharmann, "Ion induced secondary electron spectra from clean metal surfaces", *Nucl. Instrum. Methods Phys. Res., Sect. B,* vol. 18, pp. 561-565, 1987. doi:10.1016/S0168-583X(86)80088-X

[18] SRIM - The Stopping and Range of Ions in Matter http://www.srim.org